chemistry

MDPI

Communication

Exploring the Potential Energy Surface of Medium-Sized Aromatic Polycyclic Systems with Embedded Planar Tetracoordinate Carbons: A Guided Approach

Diego Inostroza [1,2], Luis Leyva-Parra [1,2], Osvaldo Yañez [3], Andrew L. Cooksy [4], Venkatesan S. Thimmakondu [4,*] and William Tiznado [1,*]

1 Centro de Química Teórica & Computacional (CQT&C), Departamento de Ciencias Químicas, Facultad de Ciencias Exactas, Universidad Andrés Bello, Avenida República 275, Santiago 8370146, Chile; dinostro92@gmail.com (D.I.); l.leyvaparra@uandresbello.edu (L.L.-P.)
2 Programa de Doctorado en Fisicoquímica Molecular, Facultad de Ciencias Exactas, Universidad Andrés Bello, Avenida República 275, Santiago 8370146, Chile
3 Núcleo de Investigación de Data Science, Facultad de Ingeniería y Negocios, Universidad de las Américas, Santiago 7500000, Chile; oyanez@udla.cl
4 Departament of Chemistry and Biochemistry, San Diego State University, San Diego, CA 92182-1030, USA; acooksy@sdsu.edu
* Correspondence: vthimmakondusamy@sdsu.edu (V.S.T.); wtiznado@unab.cl (W.T.)

Abstract: This study scrutinizes the complexities of designing and exploring the potential energy surfaces of systems containing more than twenty atoms with planar tetracoordinate carbons (ptCs). To tackle this issue, we utilized an established design rule to design a Naphtho [1,2-b:3,4-b′:5,6-b″:7,8-b‴]tetrathiophene derivative computationally. This process began with substituting S atoms with CH^- units, then replacing three sequential protons with two Si^{2+} units in the resultant polycyclic aromatic hydrocarbon polyanion. Despite not representing the global minimum, the newly designed Si_8C_{22} system with four ptCs provided valuable insights into strategic design and potential energy surface exploration. Our results underscore the importance of employing adequate methodologies to confirm the stability of newly designed molecular structures containing planar hypercoordinate carbons.

Keywords: planar tetracoordinate carbon; silicon-carbon clusters; global minima; DFT computations; chemical bonding analysis; aromaticity

check for updates

Citation: Inostroza, D.; Leyva-Parra, L.; Yañez, O.; Cooksy, A.L.; Thimmakondu, V.S.; Tiznado, W. Exploring the Potential Energy Surface of Medium-Sized Aromatic Polycyclic Systems with Embedded Planar Tetracoordinate Carbons: A Guided Approach. *Chemistry* **2023**, *5*, 1535–1545. https://doi.org/10.3390/chemistry5030105

Academic Editor: Andrea Peluso

Received: 9 June 2023
Revised: 4 July 2023
Accepted: 5 July 2023
Published: 11 July 2023

Copyright: © 2023 by the authors. Licensee MDPI, Basel, Switzerland. This article is an open access article distributed under the terms and conditions of the Creative Commons Attribution (CC BY) license (https://creativecommons.org/licenses/by/4.0/).

1. Introduction

In the past five decades, the scientific community has witnessed remarkable progress in understanding and exploring compounds containing planar hypercoordinate carbons (p-hyp-Cs) [1–23]. These intriguing compounds are characterized by carbon atoms connected to a minimum of four in-plane atoms. Despite the initial skepticism due to their violation of the van't Hoff and Le Bel's rules, which favor the tetrahedral configuration of tetracoordinate carbon compounds [24,25], researchers have made significant strides in this field.

The exploration of compounds with p-hyp-Cs can be traced back to 1968, when Monkhorst first proposed the CH_4 transition state planar structure involved in the stereomutation of methane [26]. In 1970, Hoffmann and his team showed that the stability of the planar tetracoordinate carbon (ptC) structure could be enhanced electronically [27]. This was achieved by substituting the planar methane H atoms with either σ electron donors, which improved their involvement in electron-deficient σ bonds, or π acceptors, which helped to distribute the unfavorable lone pair of the central atom. This led to the conceptualization of various molecular prototype architectures. In 1976, Collins and his colleagues theoretically introduced the first ptC-containing molecule, 1,1-dilithiocyclopropane [1].

This was followed by the unintentional synthesis of the first ptC-containing molecule by Cotton and Millar a year later [28], marking a significant milestone in this field. These studies began a journey leading to numerous discoveries and advancements.

Inspired by the concepts offered by Hoffman and coworkers, our group proposed a method for constructing ptC global minima (GM). This method centered around substituting three consecutive protons from an aromatic hydrocarbon with two E^{2+} dications, where E represents elements from Silicon (Si) to Lead (Pb) [29]. This substitution was designed to preserve the π-aromatic circuits inherent in the parent aromatic hydrocarbons. This strategy was initially tested on derivatives of small aromatic hydrocarbons, each featuring one or two ptCs [23,29–35]. A striking feature of these ptC systems is their global π-aromaticity and three-center, two-electron (3c-2e) E-ptC-E σ-bonds that display a localized σ-aromaticity. Significantly, electron deficiency and planar hypercoordination foster the formation of multicentric σ-bonds. This phenomenon is evident in planar hexacoordinate silicon, which achieves stability exclusively through delocalized σ-bonds. These bonds are induced by a combination of electron deficiency and specific quantum confinement conditions [36,37].

Exploring the potential energy surfaces (PES) of p-hyp-Cs species is essential to ensuring them as GM structures [21,23,30,34], thus supporting their experimental viability (at least in gas phase experiments) [14,38]. Consequently, devising methods to assist with PES exploration is vital for discovering new viable p-hyp-C species [39–44]. Experimentally, gaseous species are spectroscopically characterized; however, theoretical research remains indispensable in gaining insights into these compounds' structural and electronic structures, especially for identifying the lowest-energy structure (GM) and other relevant structures for matching between the computed and experimental spectrum, thus allowing for a structural elucidation of the compound identified in the gas cloud [45].

In the study of p-hyp-C systems, the employment of stochastic and evolutionary algorithms is common for locating the lowest-energy structures amongst the plethora of structural possibilities, thereby improving our understanding of the stability and reactivity of p-hyp-Cs compounds [21,23,29,46,47]. Numerous GM structures have been reported, including planar tetracoordinate, pentacoordinate, and hexacoordinate carbon structures [14,19,20,22,48,49]. However, the efficiency of search algorithms decreases with an increasing system size due to the exponential growth of the local minima to be visited [50,51]. Systems exceeding 20 atoms could present substantial challenges and these difficulties are further amplified when they comprise more than two elements, such as Si, C, and H in the current study. Therefore, an important question arises, how to explore the PES of candidates for GMs with p-hyp-Cs with more than 20 atoms?

In this study, we apply the design rule for systems with ptCs, as mentioned above, to the design of a Naphtho[1,2-b:3,4-b′:5,6-b″:7,8-b‴]tetrathiophene derivative (see Scheme 1), chosen for its aromatic peripheral pentagonal rings. Moreover, a similar strategy was employed last year, beginning with the [6]radialene benzo [1,2-c:3,4-c0:5,6-c00]trithiophene, which enabled us to design a GM harboring three ptCs [29]. The system we design here, Si_8C_{22}, has an isomer with four ptCs that exhibits aromaticity but does not correspond to the GM. Nevertheless, examining this system has been beneficial for testing the design rule and a guided strategy for exploring its PES, given the complexity of this task for such a large system using conventional techniques.

Consequently, our results emphasize the importance of employing the appropriate methodologies to validate the thermodynamic and kinetic stability of newly computationally designed structures containing p-hyp-Cs.

2. Computational Details

Our guided exploration of the PES of the Si_8C_{22} started using the coronene ($C_{24}H_{12}$) as a starting structural template, applying a dual-stage atomic exchange process. Initially, a hydrogen-to-silicon atomic substitution was executed, succeeded by a swap, where four silicon and two carbon atoms were removed to achieve the intended stoichiometry (Refer to Figure 3). Employing the AM1 method [52], we methodically scrutinized an exhaus-

tive set of 993 structures through single-point computations to pinpoint energy-favored structures. Isomers displaying energies beneath 50 kcal·mol^{-1} underwent subsequent geometric optimization at the PBE0 [53]/SDDAll [54–58] level. Then, the structures maintaining energies below 30 kcal·mol^{-1} were refined at the PBE0-D3 [59]/Def2-TZVP [60] and ωb97XD [61]/Def2-TZVP levels for comparative purposes (Figure S1), complemented by vibrational frequency assessments to affirm their status as true PES minima. Both methods render similar descriptions of relative energies; they accurately identified the putative global minimum. Hence, our analysis will be anchored on the PBE0-D3 method, given its computational efficiency and cost effectiveness. Additionally, targeted mutations were performed on the two best systems of the described method. All these calculations were performed with the Gaussian16 (Revision B.01) program [62].

We computed the current densities utilizing the GIMIC program [63,64] that implements the gauge-included atomic orbital (GIAO) method [65] at the PBE0-D3/Def2-TZVP level, considering an external magnetic field oriented perpendicular to the molecular plane. In our analysis, diatropic (aromatic) and paratropic (antiaromatic) ring currents circulated clockwise and counterclockwise, respectively. The visualization of these currents was performed with the Paraview 5.10.0 software [66,67], and the ring current strength (RCS) was determined after considering various rectangular integration planes that intersected the bonds of interest, originating from the center of the rings (Refer to Figures S2 and S3). The GIMIC program's integration process employed the two-dimensional Gauss–Lobatto algorithm [68]. Positive and negative RCS values represented the diatropic (aromatic) and paratropic (antiaromatic) ring currents, respectively, while values near zero indicated a non-aromatic character [69]. The different ring current circuits were determined by analyzing the current strength profiles across the integration planes (see Figures S2 and S3), following a strategy previously proposed elsewhere [69–71].

Chemical bonding analyses employed several methods: Wiberg bond indices (WBI) [72], a natural population analysis (NPA) [73], and the adaptive natural density partitioning method (AdNDP) [74,75]. These methodologies are anchored in the natural bond orbital (NBO) method and were executed using the wavefunction derived at the PBE0-D3/Def2-TZVP level. WBI and NPA computations were facilitated with the NBO 6.0 code [76], while the AdNDP analysis was carried out with Multiwfn 3.8 [77]. The molecular structure and AdNDP orbitals were visualized using CYLview 2.0 [78] and VMD 1.9.3 [79].

3. Results and Discussion

3.1. Design of the Si_8C_{22} Cluster Incorporating Four ptCs

This research delves into the intricate processes of designing and examining the PES of polycyclic systems comprising over twenty atoms featuring ptCs. To address this challenge, we employed a proven design principle [23,29–35] to computationally formulate a derivative of Naphtho[1,2-b:3,4-b′:5,6-b″:7,8-b‴]tetrathiophene. This design procedure initiated substituting sulfur atoms with CH^- units. Then, a sequential triplet of protons was replaced with a pair of Si^{2+} units within the resulting polycyclic aromatic hydrocarbon polyanion (see Scheme 1).

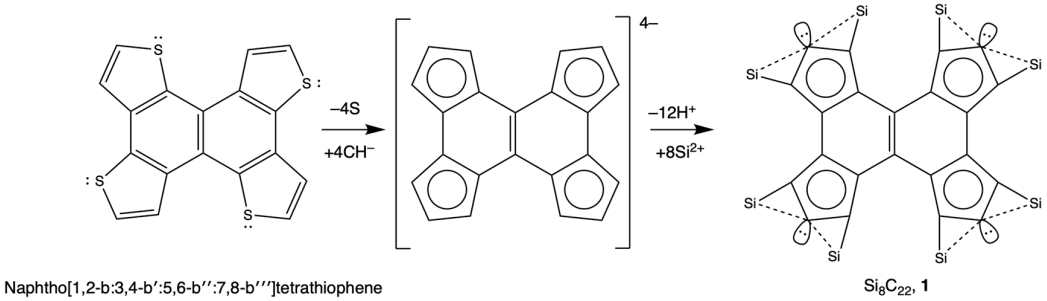

Scheme 1. Design of Si_8C_{22} ptC system starting from the Naphtho [1,2-b:3,4-b′:5,6-b″:7,8-b‴]tetrathiophene (**left**) to build $C_{22}H_{12}{}^{4-}$ and finally the ptC candidate (**right**).

Despite not achieving the global minimum (GM), the resultant cluster (**1**) was a local minimum on the PES. This allowed us to assess a simple but effective strategy to explore its PES (see below). Our findings accentuate the necessity of rigorous methodologies for validating the stability of novel structures featuring p-hyp-Cs.

A crucial prerequisite for the design of ptC-embedded aromatic rings is their inherent aromatic character. A recurring trait among the previously reported global minima (GMs) of these systems includes global, semilocal, and local π-aromaticity, with the latter two presenting in fused rings, supplemented by local σ-aromaticity provided by the delocalization of two electrons in the E-ptC-E delocalized bond, where E represents Si in this study. Thus, our analysis necessitated an in-depth evaluation of this aromaticity. To accomplish this, we assessed the magnetically induced current density. We employed current strength profiles to identify the ring current circuits and their respective strengths (nA/T), as depicted in Figure 1, following a strategy established previously [69–71].

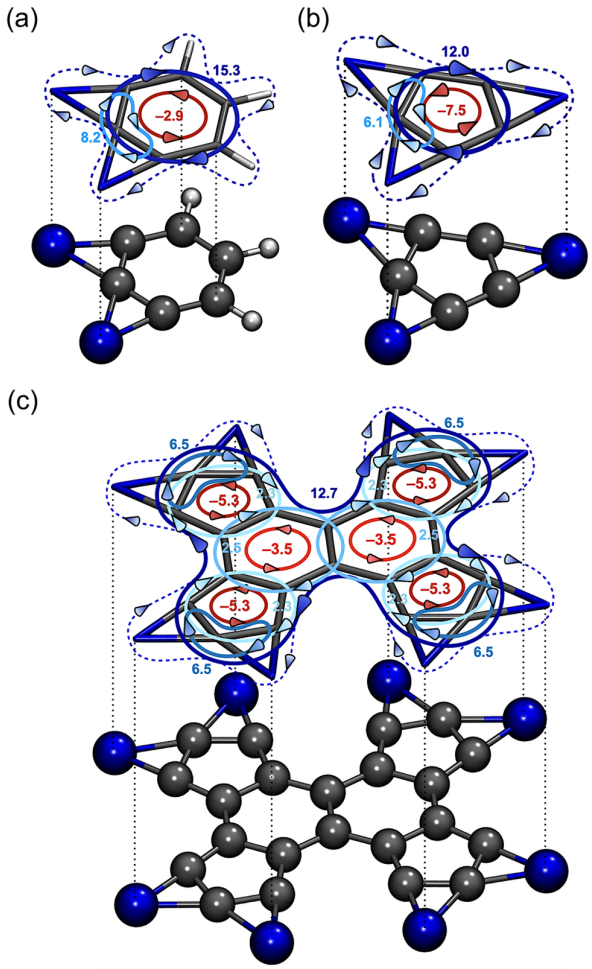

Figure 1. Schematic depiction of the identified ring current circuits (noted with their corresponding strengths in nA/T) for aromatic hydrocarbon derivatives featuring ptCs. Subfigures include: (**a**) benzene derivative ($Si_2C_6H_3^+$), (**b**) cyclopentadienyl anion derivative (Si_3C_5), and (**c**) Naphtho [1,2-b:3,4-b′:5,6-b″:7,8-b‴]tetrathiophene derivative(Si_8C_{22}).

For comparative purposes, Figure 1 also presents analyses for two formerly reported systems, one derived from benzene ($Si_2C_6H_2^+$) and another from cyclopentadienyl anion (Si_3C_5). Notably, these monocyclic rings displayed a pronounced diatropic ring current (15.3 and 12.0 nA/T), distributed predominantly around the carbon rings. Local diatropic ring currents around ptC (8.2 and 6.1 nA/T), possibly linked with local Si-ptC-Si delocalization, and paratropic ring currents at the molecular rings' center, albeit less intense,

were also discernible. These observations align with those reported earlier for these systems [30–33]. System **1**'s current density analysis revealed a strong diatropic global ring current (12.7 nA/T) and much fainter local diatropic ring currents (2.3 and 2.5 nA/T). Local currents around the ptCs and weak paratropic local currents within the local rings were also identified. Therefore, these findings affirm the robust aromatic character of system **1** following our design strategy.

However, affirming system **1** as the most stable structure for the Si_8C_{22} combination requires further verification. This validation can only be achieved by comprehensively scanning the PES of the Si_8C_{22} cluster, as elucidated in the subsequent section.

Our previous analysis revealed that the magnetic response analysis of compound **1** identified it as an aromatic system. However, what can we infer about this system from the perspective of its chemical bonding? The Adaptive Natural Density Partitioning (AdNDP) analysis offered an instructive portrayal of the chemical bonding within this species. Figure 2 depicts the AdNDP technique uncovered the lone-electron pairs on each Si atom, the C-C σ-bonds forming the C_{22} backbone, and the C-Si σ-bonds linking the C-periphery with the Si atoms. Additionally, it unveiled the delocalized Si-ptC-Si three-center two-electron (3c-2e) σ-bonds, a defining feature of these species.

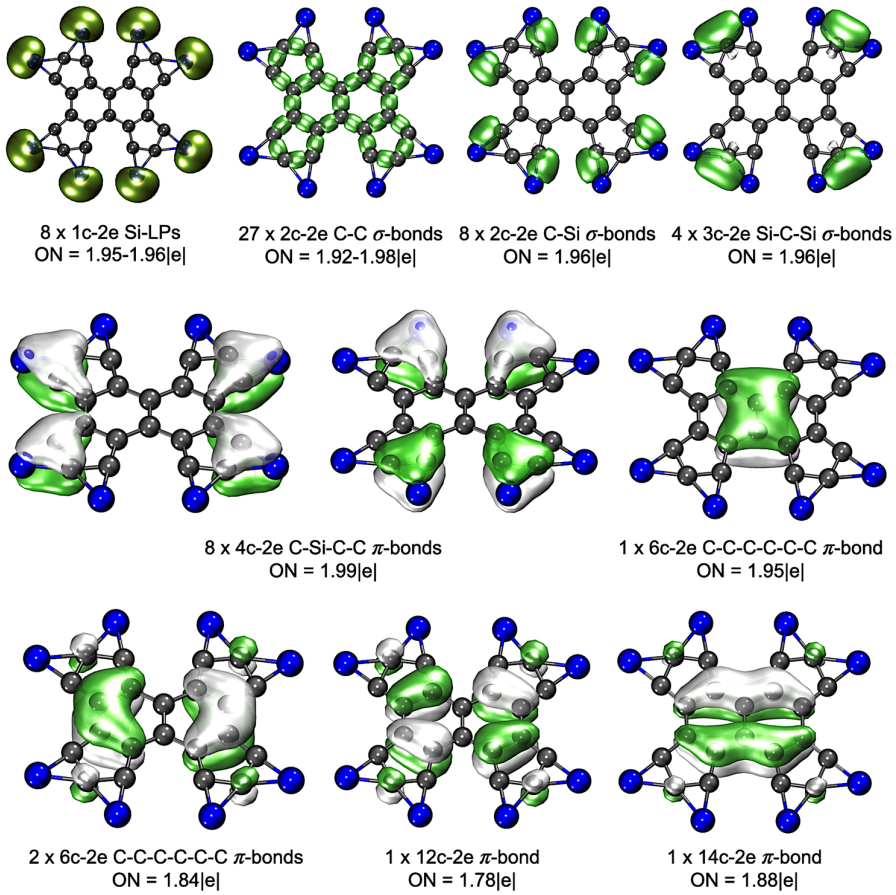

Figure 2. AdNDP analysis of **1** at the PBE0-D3/Def2-TZVP level. ON stands for occupation number. Carbon = gray, silicon = blue.

Moreover, 13 delocalized π-bonds accounting for 26 π-electrons were spread across the system. If one were to draw parallels with the current analysis, these could be partitioned into local and global groups, adhering, in both cases, to Hückel's 4n + 2 rule for aromatic systems, demonstrating their aromaticity. Thus, the AdNDP analysis confirmed that compound **1** maintained the bonding patterns observed in its predecessors, featuring ptCs integrated into an aromatic ring. This interpretation of the chemical bonding also agrees with the Wiberg bond index (WBI) analysis, as reported in Figure S4.

3.2. Potential Energy Surface Exploration of the Si_8C_{22} Cluster

As commented in the introduction, exploring the PES of medium-sized clusters using commonly implemented methods such as genetic algorithms or stochastic procedures is challenging due to the computational resources required, which many research groups might find prohibitive. This is because many candidate structures need to be evaluated and optimized locally, i.e., using density functional theory (DFT) methods and an adequate basis set.

To overcome these hurdles, we leveraged what is commonly referred to as "chemical intuition", using structural and chemical bonding information from prior studies on analogous systems to generate our candidate population. However, the success of strategies based on chemical intuition for exploring the PES of atomic clusters depends on the information used as a guide. In the past, we used the best minima derived from a stochastic search or evolutionary methods, which were subsequently slightly altered (moving atoms to generate a new structure) [80]. With this approximation, we enriched the variety of the local minima close in energy to the GM by identifying missing structures in the evolutive or stochastic search. Additionally, in the case of systems featuring p-hyp-Cs embedded in polycyclic aromatic hydrocarbons, we succeeded by performing substitutions and permutations on related and well-characterized polycyclic hydrocarbon structures to the system under study [29]. This method allowed sampling a wide range of polycyclic structures with randomness introduced by the permutations and substitutions. Thus, we will employ this strategy here.

It is crucial to mention that the used approach is successful only when we ensure that we sample the correct region of the PES, i.e., where the global minimum should ideally be found. While we cannot guarantee this 100%, our prior studies suggest it is an adequate method for this system. Building on these considerations, we illustrate the procedure employed for the PES exploration of Si_8C_{22} in Figure 3. We selected coronene ($C_{24}H_{12}$) as the starting template. We replaced the H atoms with Si, resulting in 12 Si atoms, from which we randomly removed 4 Si atoms and 2 C atoms to fulfill the desired elemental composition. Using this procedure, we generated 993 structures whose energy was computed using a semiempirical method; then, the best structures in a range of 50 kcal·mol^{-1} were optimized via a DFT method using a small basis set. Finally, we refined the best structures within a 30 kcal·mol^{-1} range at a higher level (for more details on the used methods, refer to the computational methods section). Figure 3 displays the best structures identified through our exploration. This approach allowed for a thorough yet resource-conscious exploration of the PES of Si_8C_{22}, offering valuable insights into the energetically preferred structures for this combination. Regrettably, structure **1** presented significantly higher in energy than the most favorable structure identified for the Si_8C_{22} combination (67 kcal·mol^{-1} above the putative global minimum). Revise the XYZ file in the Supplementary Materials for a detailed look at the structures and their relative energies. Nevertheless, this study underscores the essentiality of employing suitable techniques to ascertain that the designed cluster corresponds to the global minimum. This prerequisite critically influences its potential viability in the gas phase.

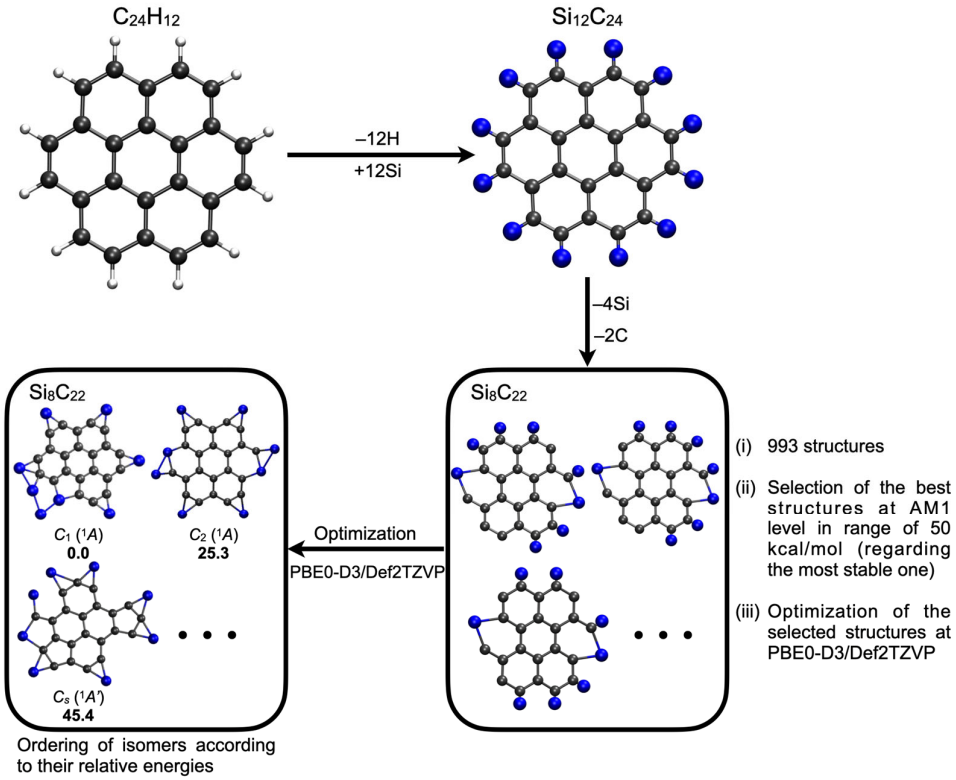

Figure 3. Schematic representation of the strategic approach for exploring the Si_8C_{22} cluster's potential energy surface.

An intriguing question that persists is why **1** is not a good minimum on the potential energy surface (PES). A plausible explanation may be uncovered by examining its computationally designed structural counterpart, the $C_{22}H_{12}^{4-}$ tetra-anion, which is stabilized by four Li^+ counterions. As reported in Cartesian coordinates (Table S1), the C_{22} skeleton in $Li_4C_{22}H_{12}$ does not lay flat, in contrast to the planar configuration in system **1**, possibly due to the rigidity imparted by the bridged Si-C bonds. Consequently, this flatness could strain the C_{22} skeleton, ultimately rendering the structure of **1** with four ptCs energetically unfavorable.

4. Conclusions

In this research, we utilized a previously suggested strategy to design a cluster, termed **1**, with the formula of Si_8C_{22}, featuring four ptCs. We adopted Naphtho[1,2-b:3,4-b′:5,6-b″:7,8-b‴]tetrathiophene as the base structure, wherein sulfur atoms were initially replaced with CH^- units. Subsequently, two Si^{2+} units replaced three sequential protons. Although this strategy has been proven successful in designing global minima featuring ptCs in the past, our findings demonstrated that **1** does not represent the global minimum. Instead, it is a local minimum, positioned over 67 kcal·mol^{-1} above the lowest-energy structure identified in this study.

An essential contribution of our work lies in assessing a novel yet straightforward methodology for exploring such systems' PES, using known polycyclic hydrocarbons as template structures. Specifically, we used coronene, which facilitated evaluating a series of designs through the substitution, elimination, and permutation of atoms.

The reliability of the minima identified through this approach is corroborated by earlier studies, where it was compared with evolutionary methods. Our findings underscore the significance of employing appropriate ways to navigate the PES when designing structures with planar hypercoordinate carbons, which is particularly pertinent for intermediate-sized forms, like **1**, where conventional stochastic or evolutionary methods can be challenging

to implement. It should be noted that the manual approach may be subject to biases that obstruct identifying the best structures.

Supplementary Materials: The following are available online at https://www.mdpi.com/article/10.3390/chemistry5030105/s1, Figure S1: Comparison between Si_8C_{22} isomers energy at PBE0-D3/Def2-TZVP and ωb97XD/Def2-TZVP levels. Figure S2: Vector plots visualization of the current density in diverse planes of the Si_3C_5, $Si_2C_6H_3^{+,}$ and Si_8C_{22} clusters. Diatropic currents are assumed to circle clockwise. Figure S3: Top view of integration planes considered to average the profile RCS for Si_3C_5, $Si_2C_6H_3^+$, and Si_8C_{22} (up) and the RCS pro-files along the different integration planes (down). Figure S4: Bond length in (black), natural charges (red and blue), and Wiberg bond indices (green) for Si_8C_{22} at the PBE0-D3/Def2-TZVP level of theory. The XYZ file includes the top isomers identified in our search and their corresponding relative energies, all computed at the PBE0-D3/Def2-TZVP level.

Author Contributions: Conceptualization, W.T., V.S.T., L.L.-P. and D.I.; methodology, D.I., O.Y. and V.S.T.; software, D.I. and O.Y.; validation, W.T., V.S.T. and L.L.-P.; formal analysis, W.T., A.L.C. and L.L.-P.; investigation, W.T., V.S.T., A.L.C. and D.I.; resources, W.T., V.S.T. and A.L.C.; data curation, V.S.T., L.L.-P., D.I. and O.Y.; writing—original draft preparation, W.T., L.L.-P. and D.I.; writing—review and editing, all authors; visualization, W.T., O.Y., L.L.-P. and D.I.; supervision, W.T. and V.S.T.; project administration, W.T. and D.I.; funding acquisition, W.T. All authors have read and agreed to the published version of the manuscript.

Funding: We thank the financial support of the National Agency for Research and Development (ANID) through FONDECYT project 1211128 (W.T.) and National Agency for Research and Development (ANID)/Scholarship Program/BECAS DOCTORADO NACIONAL/2019-21190427 (D.I.). National Agency for Research and Development (ANID)/Scholarship Program/BECAS DOCTORADO NACIONAL/2020-21201177 (L.L.-P.). Powered@NLHPC: This research was partially supported by the supercomputing infrastructure of the NLHPC (ECM-02). Computational support provided at the SDSU (for V.S.T. and A.L.C.) by DURIP Grant W911NF-10-1-0157 from the U.S. Department of Defense and by NSF CRIF Grant CHE-0947087 is gratefully acknowledged.

Data Availability Statement: All data can be obtained in the Supplementary Information.

Conflicts of Interest: The authors declare no conflict of interest.

References

1. Collins, J.B.; Dill, J.D.; Jemmis, E.D.; Apeloig, Y.; Schleyer, P.V.; Seeger, R.; Pople, J.A. Stabilization of Planar Tetracoordinate Carbon. *J. Am. Chem. Soc.* **1976**, *98*, 5419–5427. [CrossRef]
2. Erker, G. Planar-Tetracoordinate Carbon: Making Stable Anti-van′t Hoff/LeBel Compounds. *Comments Inorg. Chem.* **1992**, *13*, 111–131. [CrossRef]
3. Rottger, D.; Erker, G. Compounds containing planar-tetracoordinate carbon. *Angew. Chem. Int. Edit.* **1997**, *36*, 813–827. [CrossRef]
4. Siebert, W.; Gunale, A. Compounds containing a planar-tetracoordinate carbon atom as analogues of planar methane. *Chem. Soc. Rev.* **1999**, *28*, 367–371. [CrossRef]
5. Exner, K.; Schleyer, P.V.R. Planar hexacoordinate carbon: A viable possibility. *Science* **2000**, *290*, 1937–1940. [CrossRef] [PubMed]
6. Merino, G.; Méndez-Rojas, M.A.; Beltrán, H.I.; Corminboeuf, C.; Heine, T.; Vela, A. Theoretical analysis of the smallest carbon cluster containing a planar tetracoordinate carbon. *J. Am. Chem. Soc.* **2004**, *126*, 16160–16169. [CrossRef] [PubMed]
7. Perez, N.; Heine, T.; Barthel, R.; Seifert, G.; Vela, A.; Mendez-Rojas, M.A.; Merino, G. Planar tetracoordinate carbons in cyclic hydrocarbons. *Org. Lett.* **2005**, *7*, 1509–1512. [CrossRef]
8. Keese, R. Carbon flatland: Planar tetracoordinate carbon and fenestranes. *Chem. Rev.* **2006**, *106*, 4787–4808. [CrossRef]
9. Merino, G.; Méndez-Rojas, M.A.; Vela, A.; Heine, T. Recent advances in planar tetracoordinate carbon chemistry. *J. Comput. Chem.* **2007**, *28*, 362–372. [CrossRef]
10. Vela, A.; Méndez-Rojas, M.A.; Merino, G. Theoretical design of electronically stabilized molecules containing planar tetracoordinate carbons. In *Theoretical and Computational Chemistry*; Elsevier: Amsterdam, The Netherlands, 2007; Volume 19, pp. 251–267.
11. Pei, Y.; An, W.; Ito, K.; Schleyer, P.V.R.; Zeng, X.C. Planar pentacoordinate carbon in CAl_5^+: A global minimum. *J. Am. Chem. Soc.* **2008**, *130*, 10394–10400. [CrossRef]
12. Perez-Peralta, N.; Sanchez, M.; Martin-Polo, J.; Islas, R.; Vela, A.; Merino, G. Planar tetracoordinate carbons in cyclic semisaturated hydrocarbons. *J. Org. Chem.* **2008**, *73*, 7037–7044. [CrossRef] [PubMed]
13. Li, Y.; Liao, Y.; Chen, Z. Be_2C monolayer with quasi-planar hexacoordinate carbons: A global minimum structure. *Angew. Chem. Int. Ed.* **2014**, *53*, 7248–7252. [CrossRef] [PubMed]
14. Yang, L.M.; Ganz, E.; Chen, Z.; Wang, Z.X.; Schleyer, P.V.R. Four decades of the chemistry of planar hypercoordinate compounds. *Angew. Chem. Int. Ed.* **2015**, *54*, 9468–9501. [CrossRef] [PubMed]

15. Wang, Y.; Li, F.; Li, Y.; Chen, Z. Semi-metallic Be_5C_2 monolayer global minimum with quasi-planar pentacoordinate carbons and negative Poisson's ratio. *Nat. Commun.* **2016**, *7*, 11488. [CrossRef] [PubMed]
16. Cui, Z.-H.; Vassilev-Galindo, V.; Cabellos, J.L.; Osorio, E.; Orozco, M.; Pan, S.; Ding, Y.-H.; Merino, G. Planar pentacoordinate carbon atoms embedded in a metallocene framework. *Chem. Commun.* **2017**, *53*, 138–141. [CrossRef] [PubMed]
17. Liu, C.-S.; Zhu, H.-H.; Ye, X.-J.; Yan, X.-H. Prediction of a new BeC monolayer with perfectly planar tetracoordinate carbons. *Nanoscale* **2017**, *9*, 5854–5858. [CrossRef] [PubMed]
18. Pan, S.; Cabellos, J.L.; Orozco-Ic, M.; Chattaraj, P.K.; Zhao, L.; Merino, G. Planar pentacoordinate carbon in CGa 5+ derivatives. *Phys. Chem. Chem. Phys.* **2018**, *20*, 12350–12355. [CrossRef]
19. Vassilev-Galindo, V.; Pan, S.; Donald, K.J.; Merino, G. Planar pentacoordinate carbons. *Nat. Rev. Chem.* **2018**, *2*, 0114. [CrossRef]
20. Guo, J.-C.; Feng, L.-Y.; Barroso, J.; Merino, G.; Zhai, H.-J. Planar or tetrahedral? A ternary 17-electron $CBe_5H_4^+$ cluster with planar pentacoordinate carbon. *Chem. Commun.* **2020**, *56*, 8305–8308. [CrossRef]
21. Wang, M.-H.; Dong, X.; Ding, Y.-H.; Cui, Z.-H. Avoided spin coupling: An unexpected σ–σ diradical in global planar pentacoordinate carbon. *Chem. Commun.* **2020**, *56*, 7285–7288. [CrossRef]
22. Leyva-Parra, L.; Diego, L.; Yañez, O.; Inostroza, D.; Barroso, J.; Vásquez-Espinal, A.; Merino, G.; Tiznado, W. Planar hexacoordinate carbons: Half covalent, half ionic. *Angew. Chem. Int. Ed.* **2021**, *60*, 8700–8704. [CrossRef] [PubMed]
23. Leyva-Parra, L.; Inostroza, D.; Yañez, O.; Cruz, J.C.; Garza, J.; García, V.; Tiznado, W. Persistent planar tetracoordinate carbon in global minima structures of silicon-carbon clusters. *Atoms* **2022**, *10*, 27. [CrossRef]
24. Van't Hoff, J.H. A suggestion looking to the extension into space of the structural formulas at present used in chemistry, and a note upon the relation between the optical activity and the chemical constitution of organic compounds. *Arch. Neerl. Sci. Exactes Nat.* **1874**, *9*, 445–454.
25. Le Bel, J.A. Sur les relations qui existent entre les formules atomiques des corps organiques et le pouvoir rotatoire de leurs dissolutions. *Bull. Soc. Chim. Fr* **1874**, *22*, 337–347.
26. Monkhorst, H. Activation energy for interconversion of enantiomers containing an asymmetric carbon atom without breaking bonds. *Chem. Commun.* **1968**, *18*, 1111–1112. [CrossRef]
27. Hoffmann, R.; Alder, R.W.; Wilcox, C.F. Planar Tetracoordinate Carbon. *J. Am. Chem. Soc.* **1970**, *92*, 4992–4993. [CrossRef]
28. Cotton, F.A.; Millar, M. Probable Existence of a Triple Bond between 2 Vanadium Atoms. *J. Am. Chem. Soc.* **1977**, *99*, 7886–7891. [CrossRef]
29. Inostroza, D.; Leyva-Parra, L.; Vásquez-Espinal, A.; Contreras-García, J.; Cui, Z.-H.; Pan, S.; Thimmakondu, V.S.; Tiznado, W. E 6 C 15 (E = Si–Pb): Polycyclic aromatic compounds with three planar tetracoordinate carbons. *Chem. Commun.* **2022**, *58*, 13075–13078. [CrossRef]
30. Yañez, O.; Vásquez-Espinal, A.; Pino-Rios, R.; Ferraro, F.; Pan, S.; Osorio, E.; Merino, G.; Tiznado, W. Exploiting electronic strategies to stabilize a planar tetracoordinate carbon in cyclic aromatic hydrocarbons. *Chem. Commun.* **2017**, *53*, 12112–12115. [CrossRef]
31. Thimmakondu, V.S. Comment on "Exploiting electronic strategies to stabilize a planar tetracoordinate carbon in cyclic aromatic hydrocarbons" by O. Yañez et al., *Chem. Commun.* **2017**, *53*, 12112. *Chem. Commun.* **2019**, *55*, 12719–12720. [CrossRef]
32. Yanez, O.; Vasquez-Espinal, A.; Pino-Rios, R.; Ferraro, F.; Pan, S.; Osorio, E.; Merino, G.; Tiznado, W. Reply to the 'Comment on "Exploiting electronic strategies to stabilize a planar tetracoordinate carbon in cyclic aromatic hydrocarbons"' by V. S. Thimmakondu, *Chem. Commun.* **2019**, *55*, 12719–12720. *Chem. Commun.* **2019**, *55*, 12721–12722. [CrossRef] [PubMed]
33. Yañez, O.; Vásquez-Espinal, A.; Báez-Grez, R.; Rabanal-León, W.A.; Osorio, E.; Ruiz, L.; Tiznado, W. Carbon rings decorated with group 14 elements: New aromatic clusters containing planar tetracoordinate carbon. *New J. Chem.* **2019**, *43*, 6781–6785. [CrossRef]
34. Yañez, O.; Báez-Grez, R.; Garza, J.; Pan, S.; Barroso, J.; Vásquez-Espinal, A.; Merino, G.; Tiznado, W. Embedding a Planar Hypercoordinate Carbon Atom into a [4n+ 2] π-System. *ChemPhysChem* **2020**, *21*, 145–148. [CrossRef]
35. Inostroza, D.; Leyva-Parra, L.; Yañez, O.; Cruz, J.C.; Garza, J.; García, V.; Thimmakondu, V.S.; Ceron, M.L.; Tiznado, W. Si_6C_{18}: A bispentalene derivative with two planar tetracoordinate carbons. *Int. J. Quantum Chem.* **2022**, *123*, e27008.
36. Yang, L.-M.; Bacic, V.; Popov, I.A.; Boldyrev, A.I.; Heine, T.; Frauenheim, T.; Ganz, E. Two-dimensional Cu_2Si monolayer with planar hexacoordinate copper and silicon bonding. *J. Am. Chem. Soc.* **2015**, *137*, 2757–2762. [CrossRef]
37. Yang, L.-M.; Popov, I.A.; Frauenheim, T.; Boldyrev, A.I.; Heine, T.; Bačić, V.; Ganz, E. Revealing unusual chemical bonding in planar hyper-coordinate Ni_2Ge and quasi-planar Ni_2Si two-dimensional crystals. *Phys. Chem. Chem. Phys.* **2015**, *17*, 26043–26048. [CrossRef]
38. Li, X.; Zhang, H.F.; Wang, L.S.; Geske, G.D.; Boldyrev, A.I. Pentaatomic tetracoordinate planar carbon, [CAl4] 2−: A new structural unit and its salt complexes. *Angew. Chem.* **2000**, *112*, 3776–3778. [CrossRef]
39. Curtarolo, S.; Morgan, D.; Persson, K.; Rodgers, J.; Ceder, G. Predicting crystal structures with data mining of quantum calculations. *Phys. Rev. Lett.* **2003**, *91*, 135503. [CrossRef]
40. Addicoat, M.A.; Metha, G.F. Kick: Constraining a stochastic search procedure with molecular fragments. *J. Comput. Chem.* **2009**, *30*, 57–64. [CrossRef]
41. Wang, Y.; Lv, J.; Zhu, L.; Ma, Y. Crystal structure prediction via particle-swarm optimization. *Phys. Rev. B* **2010**, *82*, 094116. [CrossRef]

42. Yanez, O.; Baez-Grez, R.; Inostroza, D.; Rabanal-Leon, W.A.; Pino-Rios, R.; Garza, J.; Tiznado, W. AUTOMATON: A Program That Combines a Probabilistic Cellular Automata and a Genetic Algorithm for Global Minimum Search of Clusters and Molecules. *J. Chem. Theory Comput.* **2019**, *15*, 1463–1475. [CrossRef]
43. Yañez, O.; Inostroza, D.; Usuga-Acevedo, B.; Vásquez-Espinal, A.; Pino-Rios, R.; Tabilo-Sepulveda, M.; Garza, J.; Barroso, J.; Merino, G.; Tiznado, W. Evaluation of restricted probabilistic cellular automata on the exploration of the potential energy surface of Be6B11$^-$. *Theor. Chem. Acc.* **2020**, *139*, 41. [CrossRef]
44. Yañez, O.; Báez-Grez, R.; Inostroza, D.; Pino-Rios, R.; Rabanal-León, W.A.; Contreras-García, J.; Cardenas, C.; Tiznado, W. Kick–Fukui: A Fukui Function-Guided Method for Molecular Structure Prediction. *J. Chem. Inf. Model.* **2021**, *61*, 3955–3963. [CrossRef] [PubMed]
45. Boldyrev, A.I.; Wang, L.-S. All-Metal Aromaticity and Antiaromaticity. *Chem. Rev.* **2005**, *105*, 3716–3757. [CrossRef] [PubMed]
46. Guo, J.C.; Feng, L.Y.; Zhang, X.Y.; Zhai, H.J. Star-Like $CBe_5Au_5^+$ Cluster: Planar Pentacoordinate Carbon, Superalkali Cation, and Multifold (pi and sigma) Aromaticity. *J. Phys. Chem. A* **2018**, *122*, 1138–1145. [CrossRef]
47. Kalita, A.J.; Rohman, S.S.; Kashyap, C.; Ullah, S.S.; Guha, A.K. Double aromaticity in a $BBe_6H_6^+$ cluster with a planar hexacoordinate boron structure. *Chem. Commun.* **2020**, *56*, 12597–12599. [CrossRef]
48. Averkiev, B.B.; Zubarev, D.Y.; Wang, L.M.; Huang, W.; Wang, L.S.; Boldyrev, A.I. Carbon Avoids Hypercoordination in CB6−, CB62−, and C2B5− Planar Carbon−Boron Clusters. *J. Am. Chem. Soc.* **2008**, *130*, 9248–9250. [CrossRef]
49. Leyva-Parra, L.; Diego, L.; Inostroza, D.; Yañez, O.; Pumachagua-Huertas, R.; Barroso, J.; Vásquez-Espinal, A.; Merino, G.; Tiznado, W. Planar Hypercoordinate Carbons in Alkali Metal Decorated CE_3^{2-} and CE_2^{2-} Dianions. *Chem.–A Eur. J.* **2021**, *27*, 16701–16706. [CrossRef]
50. Stillinger, F.H. Exponential multiplicity of inherent structures. *Phys. Rev. E* **1999**, *59*, 48. [CrossRef]
51. Rossi, G.; Ferrando, R. Searching for low-energy structures of nanoparticles: A comparison of different methods and algorithms. *J. Phys. Condens. Matter* **2009**, *21*, 084208. [CrossRef]
52. Dewar, M.J.; Zoebisch, E.G.; Healy, E.F.; Stewart, J.J. Development and use of quantum mechanical molecular models. 76. AM1: A new general purpose quantum mechanical molecular model. *J. Am. Chem. Soc.* **1985**, *107*, 3902–3909. [CrossRef]
53. Adamo, C.; Barone, V. Toward reliable density functional methods without adjustable parameters: The PBE0 model. *J. Chem. Phys.* **1999**, *110*, 6158–6170. [CrossRef]
54. Fuentealba, P.; Preuss, H.; Stoll, H.; Von Szentpály, L. A proper account of core-polarization with pseudopotentials: Single valence-electron alkali compounds. *Chem. Phys. Lett.* **1982**, *89*, 418–422. [CrossRef]
55. Fuentealba, P.; Von Szentpaly, L.; Preuss, H.; Stoll, H. Pseudopotential calculations for alkaline-earth atoms. *J. Phys. B: At. Mol. Phys.* **1985**, *18*, 1287. [CrossRef]
56. Küchle, W.; Dolg, M.; Stoll, H.; Preuss, H. Ab initio pseudopotentials for Hg through Rn: I. Parameter sets and atomic calculations. *Mol. Phys.* **1991**, *74*, 1245–1263. [CrossRef]
57. Bergner, A.; Dolg, M.; Küchle, W.; Stoll, H.; Preuß, H. Ab initio energy-adjusted pseudopotentials for elements of groups 13–17. *Mol. Phys.* **1993**, *80*, 1431–1441. [CrossRef]
58. Küchle, W.; Dolg, M.; Stoll, H.; Preuss, H. Energy-adjusted pseudopotentials for the actinides. Parameter sets and test calculations for thorium and thorium monoxide. *J. Chem. Phys.* **1994**, *100*, 7535–7542. [CrossRef]
59. Grimme, S.; Antony, J.; Ehrlich, S.; Krieg, H. A consistent and accurate ab initio parametrization of density functional dispersion correction (DFT-D) for the 94 elements H-Pu. *J. Chem. Phys.* **2010**, *132*, 154104. [CrossRef]
60. Weigend, F.; Ahlrichs, R. Balanced basis sets of split valence, triple zeta valence and quadruple zeta valence quality for H to Rn: Design and assessment of accuracy. *Phys. Chem. Chem. Phys.* **2005**, *7*, 3297–3305. [CrossRef]
61. Chai, J.-D.; Head-Gordon, M. Long-range corrected hybrid density functionals with damped atom–atom dispersion corrections. *Phys. Chem. Chem. Phys.* **2008**, *10*, 6615–6620. [CrossRef]
62. Frisch, M.J.; Trucks, G.W.; Schlegel, H.B.; Scuseria, G.E.; Robb, M.A.; Cheeseman, J.R.; Scalmani, G.; Barone, V.; Petersson, G.A.; Nakatsuji, H.; et al. *Gaussian 16 Rev. B.01*; Gaussian, Inc.: Wallingford, CT, USA, 2016.
63. Jusélius, J.; Sundholm, D.; Gauss, J. Calculation of current densities using gauge-including atomic orbitals. *J. Chem. Phys.* **2004**, *121*, 3952–3963. [CrossRef] [PubMed]
64. Fliegl, H.; Taubert, S.; Lehtonen, O.; Sundholm, D. The gauge including magnetically induced current method. *Phys. Chem. Chem. Phys.* **2011**, *13*, 20500–20518. [CrossRef] [PubMed]
65. Wolinski, K.; Hinton, J.F.; Pulay, P. Efficient implementation of the gauge-independent atomic orbital method for NMR chemical shift calculations. *J. Am. Chem. Soc.* **1990**, *112*, 8251–8260. [CrossRef]
66. Ayachit, U.; Geveci, B.; Moreland, K.; Patchett, J.; Ahrens, J. The ParaView visualization application. In *High Performance Visualization*, 1st ed.; Bethel, E.W., Childs, H., Hansen, C., Eds.; Taylor & Francis: New York, NY, USA, 2012; pp. 383–400.
67. Ayachit, U. *The Paraview Guide: A Parallel Visualization Application*; Kitware, Inc.: Clifton Park, NY, USA, 2015.
68. Abramowitz, M. *Handbook of Mathematical Functions, with Formulas, Graphs, and Mathematical Tables*; US Government Printing Office: New York, NY, USA, 1974.
69. Sundholm, D.; Fliegl, H.; Berger, R.J. Calculations of magnetically induced current densities: Theory and applications. *Wiley Interdiscip. Rev. Comput. Mol. Sci.* **2016**, *6*, 639–678. [CrossRef]
70. Sundholm, D.; Berger, R.J.; Fliegl, H. Analysis of the magnetically induced current density of molecules consisting of annelated aromatic and antiaromatic hydrocarbon rings. *Phys. Chem. Chem. Phys.* **2016**, *18*, 15934–15942. [CrossRef]

71. Inostroza, D.; García, V.; Yañez, O.; Torres-Vega, J.J.; Vásquez-Espinal, A.; Pino-Rios, R.; Báez-Grez, R.; Tiznado, W. On the NICS limitations to predict local and global current pathways in polycyclic systems. *New J. Chem.* **2021**, *45*, 8345–8351. [CrossRef]
72. Wiberg, K.B. Application of the pople-santry-segal CNDO method to the cyclopropylcarbinyl and cyclobutyl cation and to bicyclobutane. *Tetrahedron* **1968**, *24*, 1083–1096. [CrossRef]
73. Reed, A.E.; Weinstock, R.B.; Weinhold, F. Natural population analysis. *J. Chem. Phys.* **1985**, *83*, 735–746. [CrossRef]
74. Zubarev, D.Y.; Boldyrev, A.I. Developing paradigms of chemical bonding: Adaptive natural density partitioning. *Phys. Chem. Chem. Phys.* **2008**, *10*, 5207–5217. [CrossRef]
75. Zubarev, D.Y.; Boldyrev, A.I. Revealing intuitively assessable chemical bonding patterns in organic aromatic molecules via adaptive natural density partitioning. *J. Org. Chem.* **2008**, *73*, 9251–9258. [CrossRef]
76. Glendening, E.D.; Landis, C.R.; Weinhold, F. NBO 6.0: Natural bond orbital analysis program. *J. Comput. Chem.* **2013**, *34*, 1429–1437. [CrossRef] [PubMed]
77. Lu, T.; Chen, F. Multiwfn: A multifunctional wavefunction analyzer. *J. Comput. Chem.* **2012**, *33*, 580–592. [CrossRef] [PubMed]
78. Legault, C.Y. *CYLview20*; Université de Sherbrooke: Sherbrooke, QC, Canada, 2020.
79. Humphrey, W.; Dalke, A.; Schulten, K. VMD: Visual molecular dynamics. *J. Mol. Graph.* **1996**, *14*, 33–38. [CrossRef] [PubMed]
80. Thimmakondu, V.S.; Sinjari, A.; Inostroza, D.; Vairaprakash, P.; Thirumoorthy, K.; Roy, S.; Anoop, A.; Tiznado, W. Why an integrated approach between search algorithms and chemical intuition is necessary? *Phys. Chem. Chem. Phys.* **2022**, *24*, 11680–11686. [CrossRef]

Disclaimer/Publisher's Note: The statements, opinions and data contained in all publications are solely those of the individual author(s) and contributor(s) and not of MDPI and/or the editor(s). MDPI and/or the editor(s) disclaim responsibility for any injury to people or property resulting from any ideas, methods, instructions or products referred to in the content.